Available online at www.sciencedirect.com
ScienceDirect
Journal of Solid State Chemistry 180 (2007) 3450–3455
JOURNAL OF SOLID STATE CHEMISTRY
www.elsevier.com/locate/jssc

Photoluminescence properties of $La(PO_3)_3:Tb^{3+}$ under VUV excitation

Yuhua Wang*, Dan Wang

Department of Materials Science, Lanzhou University, Lanzhou 730000, China

Received 15 May 2007; received in revised form 9 August 2007; accepted 1 October 2007
Available online 13 October 2007

Abstract

$La_{1-x}(PO_3)_3:Tb_x^{3+}$ $(0<x\leqslant 0.6)$ were prepared using solid-state reaction. The vacuum ultraviolet (VUV) excitation spectrum of $La_{0.55}(PO_3)_3:Tb_{0.45}^{3+}$ indicates that the absorption of $(PO_3)_3^{3-}$ groups locates at about 163 and 174 nm and the absorption bands of $(PO_3)_3^{3-}$ groups (174 nm) and La^{3+}–O^{2-} (200 nm) and Tb^{3+} (213 nm) overlap each other. These results imply that the $(PO_3)_3^{3-}$ groups can efficiently absorb the excited energy around 172 nm and transfer the energy to Tb^{3+}. Under 172 nm excitation, the optimal photoluminescence (PL) intensity is obtained when Tb concentration reaches 0.45 and is about 71% of commercial phosphor $Zn_{1.96}SiO_4$:0.04 Mn^{2+} with chromaticity coordinates of (0.343, 0.578) and the decay time of about 4.47 ms.

Keywords: $La(PO_3)_3:Tb^{3+}$; Optical properties; Vacuum ultraviolet excitation

1. Introduction

Recently, the research on phosphors excited by vacuum ultraviolet (VUV) radiation has attracted much attention because they can be applied in plasma display panels (PDPs) and new generation of mercury-free fluorescent lamps. The VUV light consists of the Xe resonance emission line (147 nm) and the Xe_2 molecular emission band (172 nm). Under VUV excitation, most of the photons are absorbed by host crystal, and then the absorbed energy would be transferred from the host to rare-earth ions and allows them to emit visible light. Therefore, the host absorption efficiency and the energy transfer efficiency are very important for phosphors applied in VUV region.

Phosphates are promising phosphors because their anion PO_4^{3-} can efficiently absorb the energy in the region of 132–186 nm [1–7]. $Ln(PO_3)_3$ (Ln = La to Lu and Y) is one of complex polyphosphates with two different crystal structures [4,8–13]. $Ln(PO_3)_3$ with large rare-earth ions (La to Gd) crystallize in an orthorhombic crystal structure, while the others crystallize in a monoclinic crystal structure. We have investigated the PL properties of $La_{1-z}P_3O_9:Eu_z^{3+}$ $(0<z\leqslant 1)$ under 147, 172 and 254 nm excitation and found that the $P_3O_9^{3-}$ groups can efficiently absorb the excited energy around 174 nm. The optimum emission intensity of $La_{1-z}P_3O_9:Eu_z^{3+}$ $(0<z\leqslant 1)$, obtained when z reaches 1, is about 68% of $(Y,Gd)BO_3:Eu^{3+}$ under 172 nm excitation [7]. Thus we confirm that orthorhombic LaP_3O_9 is a promising host under VUV excitation and conjecture that other activator ions (such as Tb^{3+}) in this structure should have an efficient emission, too.

Tb^{3+} is used as the activator ion and doped into the host lattice. That is because the strongest emission of Tb^{3+} situates around 545 nm [14–17]. Moreover, parts of Tb^{3+} absorption locate in VUV region and overlap with the host absorption bands [15,16], so the energy can be efficiently transferred from the host to Tb^{3+} and allow Tb^{3+} to emit green light.

In this paper, we synthesize $La_{1-x}(PO_3)_3:Tb_x^{3+}$ $(0<x\leqslant 0.6)$ using solid-state reaction and investigate their PL properties under 172 nm excitation. The optimal emission is obtained when x reaches 0.45. In order to explain this concentration quenching, $Tb(PO_3)_3$ is prepared and its VUV excitation spectrum is investigated too.

2. Experimental

$La_{1-x}(PO_3)_3:Tb_x^{3+}$ $(0<x\leqslant 0.6)$ and $Tb(PO_3)_3$ are prepared by mixing stoichiometric quantities of La_2O_3

*Corresponding author. Fax: +86 931 8913554.
E-mail address: wyh@lzu.edu.cn (Y. Wang).

0022-4596/$ - see front matter © 2007 Elsevier Inc. All rights reserved.
doi:10.1016/j.jssc.2007.10.008

(99.95%), Tb_4O_7 (99.99%) and $(NH_4)_2HPO_4$ (98.5%, excess of 30 mol%). Excess of $(NH_4)_2HPO_4$ is added to compensate the evaporation loss at higher temperature. After intimately mixing the starting materials with ethanol, the obtained mixture is heated at 400 °C for 1 h and then at 700 °C for 1 h. After subsequent grinding they are fired again at 900 °C for 10 h and cooled to room temperature. Carbon powder is used to prevent the oxidization of Tb^{3+} in the preparation of these samples.

All the samples were checked by X-ray diffraction (XRD) using Rigaku diffractometer with Ni-filtered Cu$K\alpha$ radiation. The infrared (IR) absorption spectrum was measured at room temperature, using a spectrum GX FT–IR system from Perkin-Elmer.

The VUV excitation and emission spectra were measured by FLS-920T fluorescence spectrophotometer with a VM-504-type vacuum monochromator using a deuterium lamp as the lighting source. The excitation spectra were corrected with sodium salicylate, whose quantum efficiency was almost constant in 120–200 nm region. All the measurements were performed at room temperature.

3. Results and discussion

Fig. 1 shows the crystal structure of $La(PO_3)_3$. $La(PO_3)_3$ crystallizes in the orthorhombic system with space group $C222_1$. The $(PO_3)_3^{3-}$ groups are composed of three P–O tetrahedra with sharing O^{2-} corner. The P ions occupy two different crystallographic sites and form two kinds of PO_4 tetrahedra. The configuration between two PO_4 tetrahedra is different. One tetrahedron has good symmetry, and the other tetrahedron is asymmetry. The La^{3+} ions occupy only one crystallographic site and form one-dimensional

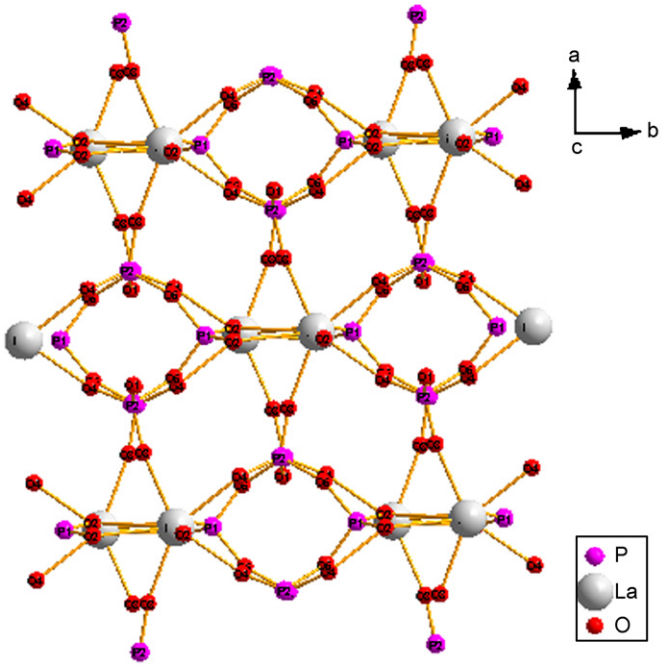

Fig. 1. Crystal structure of $La(PO_3)_3$.

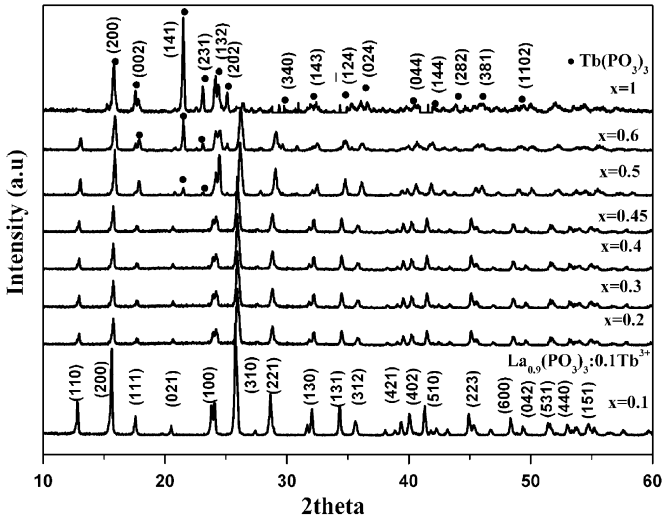

Fig. 2. XRD patterns of $La_{1-x}(PO_3)_3:Tb_x^{3+}$ ($0<x\leqslant 0.6$) and $Tb(PO_3)_3$.

sublattice of zigzag chains along c-axis. The shortest La^{3+}–La^{3+} distance in the chain is about 4.315 Å [10].

The XRD patterns of $La_{1-x}(PO_3)_3:Tb_x^{3+}$ ($0<x\leqslant 0.6$) and $Tb(PO_3)_3$ are shown in Fig. 2. The obtained samples are a single phase with orthorhombic structure when $x\leqslant 0.45$. The XRD pattern of $La_{0.9}(PO_3)_3:Tb_{0.1}^{3+}$ is indexed with the lattice parameters $a=11.21$ Å, $b=8.58$ Å, $c=7.32$ Å and $V=704.38$ Å^3, respectively. This is consistent with the JCPDF file No. 33-0717 which shows the XRD pattern of LaP_3O_9. According to the reference of the JCPDF file No. 33-0717 [10], the formula for the lanthanum metaphosphate (LaP_3O_9) would be $La(PO_3)_3$. Therefore, we use the formula $La(PO_3)_3$ throughout the text. Monoclinic $Tb(PO_3)_3$, maybe containing La^{3+}, is detected as the second phase when $x>0.45$ for the different crystal structures between $La(PO_3)_3$ and $Tb(PO_3)_3$ [9,10]. The XRD pattern of $Tb(PO_3)_3$ is indexed with the lattice parameters $a=11.27$ Å, $b=20.25$ Å, $c=10.16$ Å, $\beta=97.20°$ and $V=2290.98$ Å^3, respectively, which is in agreement with the JCPDF file No. 31-1379.

Fig. 3 shows the changes of a, b and c unit cell parameters for $La_{1-x}(PO_3)_3:Tb_x^{3+}$ ($0<x\leqslant 0.45$) as a function of the Tb^{3+} concentration x. All the lattice parameters have a tendency to decrease linearly with increasing the values of x. That is because La^{3+} ions in $La(PO_3)_3$ occupy only one crystallographic site and form LaO_8 dodecahedra with oxygen atoms [10]. In LnO_8 polyhedron, Tb^{3+} ionic radius is smaller than La^{3+} [18]. Therefore, the lattice parameters of $La_{1-x}(PO_3)_3:Tb_x^{3+}$ would decrease when Tb^{3+} substitutes for La^{3+} in $La(PO_3)_3$. This result is consistent with Vegard's law and indicates that Tb^{3+} ions have occupied La^{3+} ion sites.

Fig. 4 shows the room temperature FT–IR spectrum of $La(PO_3)_3$ in the range of 400–1600 cm^{-1}. The pattern of the stretching vibration frequencies of $La(PO_3)_3$ is similar to $Pr(PO_3)_3$ reported in Ref. [12]. This result hints that $La(PO_3)_3$ is isostructural with $Pr(PO_3)_3$. $Pr(PO_3)_3$ belongs to orthorhombic crystal structure with space group $C222_1$.

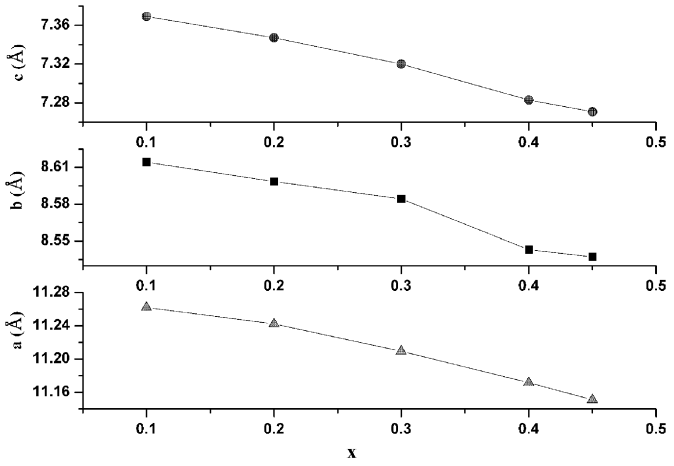

Fig. 3. Concentration dependence of a, b and c unit cell parameter for $La_{1-x}(PO_3)_3$:Tb_x^{3+} ($0<x\leqslant 0.45$).

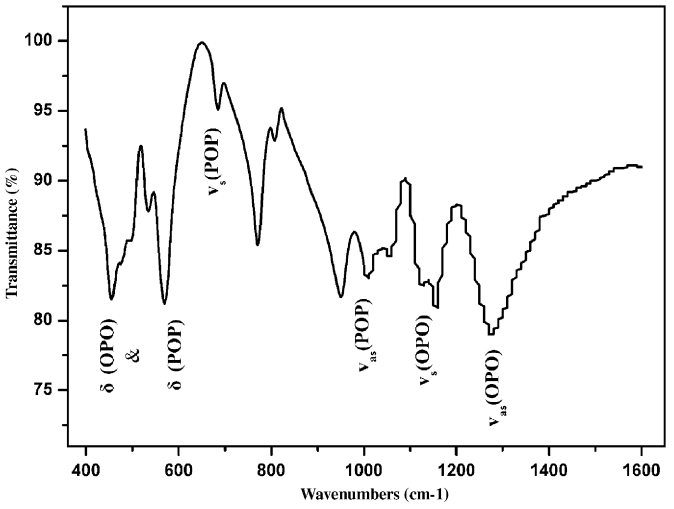

Fig. 4. Room temperature FT–IR spectrum of $La(PO_3)_3$.

In the $Pr(PO_3)_3$ structure, oxygen atoms form a PO_4 tetrahedron and a PrO_8 polyhedron. The PO_4 tetrahedra share corners to produce helical chains and the PrO_8 polyhedra share edges to form zigzag chains. This structure is consistent with the description of Fig. 1 and confirms that the writing of formula $La(PO_3)_3$ is right. The assignments of the bands and lines observed in the IR spectrum are shown in Fig. 4.

In Fig. 5 the VUV excitation spectrum of $La_{0.55}(PO_3)_3$:$Tb_{0.45}^{3+}$ (curve a) is plotted by monitoring the 545 nm emission and contains four broad bands with the maxima at 163, 174, 210 and 239 nm, respectively. The bands at 163 and 174 nm could be related to the absorption of $(PO_3)_3^{3-}$ groups. The main reasons for this assignment are shown as follows: Firstly, the VUV reflection spectra of KH_2PO_4 and $NH_4H_2PO_4$ definitely indicate that the P–O tetrahedron can absorb the energy in the region of 7–9 eV due to the transitions from group β to group δ [19]. The β is non-bonding orbital mainly composed of the O($2p\pi$) orbital and the bonding orbital between O($2p\pi$) and

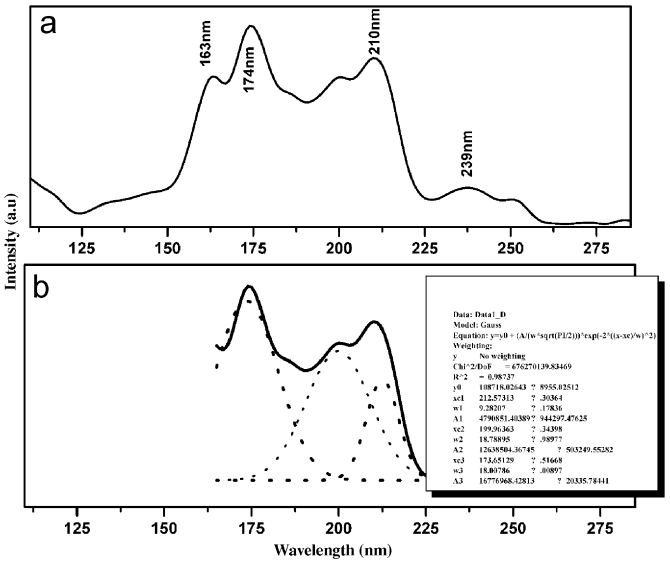

Fig. 5. Excitation spectrum of $La_{0.55}(PO_3)_3$:$Tb_{0.45}^{3+}$ in VUV region (curve a, $\lambda_{em}=545$ nm). Curve b exhibits a possible model for the band overlapping around 210 nm using Gaussian distribution curve.

Table 1
Positions of absorption band of P–O tetrahedron in some phosphates

Compound	Position of absorption band (P–O tetrahedron) (nm)	Ref.
YPO_4:Eu^{3+}	152	[2]
$LuPO_4$:Eu^{3+}	145	[2]
	151	[2]
$LaPO_4$:Eu^{3+}	159	[2],
	151	[20]
$GdPO_4$:Eu^{3+}	160	[2]
	149	[20]
$Ba_3(PO_4)_2$:Eu^{2+}	154	[6]
$Ba_3(PO_4)_2$:Eu^{3+}	165	[6]
$Ba_3(PO_4)_2$:Sm^{3+}	168	[6]
$Ba_3(PO_4)_2$:Tb^{3+}	170	[6]
LaP_3O_9:Eu^{3+}	146,174	[4]
$CaBPO_5$:RE^{3+} (RE = Ce, Sm, Eu, Eu, Tb and Dy	155	[21]
$Sr_3Gd(PO_4)_3$:Ln^{3+} (Ln = Ce, Pr and Tb)	Near 170	[22]

P($3p$). The δ is the anti-bonding orbital of P($3s$) and O($2p\sigma$). That hints that the configuration of P–O tetrahedron would greatly affect the position of the absorption band of P–O tetrahedron. Secondly, two P sites exist and form two kinds of PO_4 tetrahedra in the crystal lattice of $La(PO_3)_3$. The configuration between two PO_4 tetrahedra is different. One tetrahedron has good symmetry, and the other tetrahedron is asymmetry [10]. These structural features hint that the $(PO_3)_3^{3-}$ would have two absorption bands in the region of 7–9 eV, and the bands at 163 and 174 nm could be related to $(PO_3)_3^{3-}$ group absorption. In addition, the absorption band of P–O tetrahedron in some phosphates has been observed in VUV region (Table 1). Therefore, we ascribe the bands at 163 and 174 nm to the

absorption of $(PO_3)_3^{3-}$ groups of $La(PO_3)_3$. In the before work, the absorption bands of $P_3O_9^{3-}$ groups in LaP_3O_9:Eu^{3+} (the accurate formula is $La(PO_3)_3$:Eu^{3+}, we use $La(PO_3)_3$:Eu^{3+} instead of LaP_3O_9:Eu^{3+} in the text below) were observed at 146 and 174 nm [4]. There is a surprising positional difference for the high-energy peak. A possible reason is that the energy transfer process is different between $La(PO_3)_3$:Eu^{3+} and $La(PO_3)_3$:Tb^{3+}. Under 172 nm excitation, the excited energy is absorbed firstly by the $(PO_3)_3^{3-}$ groups which are formed by three PO_4 tetrahedra. For Eu^{3+}-doped $La(PO_3)_3$, the absorbed energy would be transferred from $(PO_3)_3^{3-}$ group to the charge transfer (CT) state of Eu^{3+}–O^{2-} and allows Eu^{3+} to emit red light. In the excited Eu^{3+}–O^{2-} group electronic charge has been removed from the oxygen ions to the central Eu^{3+} ion. This situation would influence the near PO_4 tetrahedron in the ground state in such a way that it will now take more energy to bring this PO_4 tetrahedron into the excited state, because the potential field at the O^{2-} ions of the unexcited PO_4 tetrahedron increases if the negative charge on the O^{2-} ions of the excited Eu^{3+}–O^{2-} group decreases. Moreover, two kinds of PO_4 tetrahedra exist in $La(PO_3)_3$, which indicate that the PO_4 tetrahedron near Eu^{3+} ion would be greatly affected. Therefore, parts of the $(PO_3)_3^{3-}$ absorption bands in $La(PO_3)_3$:Eu^{3+} would shift to the high-energy region. For Tb^{3+}-doped $La(PO_3)_3$, the absorbed energy is transferred from $(PO_3)_3^{3-}$ groups to the 4*f*–5*d* levels of Tb^{3+} and allows Tb^{3+} to emit green light. Thus the absorption band of $(PO_3)_3^{3-}$ group in $La_{0.55}(PO_3)_3$:$Tb_{0.45}^{3+}$ could not shift. As a result, the absorption band (163 nm) of the $(PO_3)_3^{3-}$ group in $La_{0.55}(PO_3)_3$:$Tb_{0.45}^{3+}$ locates at lower energy region in comparison with that (146 nm) in $La(PO_3)_3$:Eu^{3+}. The similar phenomenon has also been observed in the VUV excitation spectra of $Ba_3(PO_4)_2$:*RE* (*RE* = Eu^{3+}, Eu^{2+}, Sm^{3+}, Tb^{3+}) [6]. However, because the mechanisms of VUV excitation and energy transfer are not clear, more work is required.

The asymmetrical form of the broad band around 210 nm implies that it could be the overlapping of several bands. Using the Gaussian distribution curve to model this band, the result exhibits that this band is the overlapping of three bands with the maxima at about 174, 200 and 213 nm, respectively (curve *b* in Fig. 5). The band at 174 nm is one of the absorption bands of $(PO_3)_3^{3-}$ groups as mentioned above. In view of the position of the 4*f*–5*d* transition bands of Tb^{3+} in other phosphates shown in Table 2, the band at 213 nm should be assigned to the 4*f*–5*d* transition of Tb^{3+}. The band at 200 nm could correlate with the CT absorption of La^{3+}–O^{2-} due to Ref. [4]. According to Ref. [26], the spin-allowed *f*–*d* transition should be strong with higher energy and the spin-forbidden *f*–*d* transition is weak with lower energy. Therefore, we ascribe the bands at about 239 nm as well as 213 nm to the spin-forbidden and spin-allowed 4*f*–5*d* transition of Tb^{3+}, respectively.

Table 2
Positions of 4*f*–5*d* transitions bands of Tb^{3+} in some phosphates

Compound	Spin-allowed transition (nm)	Spin-forbidden transition (nm)	Ref.
YPO_4:Tb^{3+}	187; 226	267	[23]
$GdPO_4$:Tb^{3+}	204;	221	[24]
$Ba_3BP_3O_{12}$:Tb^{3+}	220;	260	[25]
$NaGdFPO_4$:Tb^{3+}	220;	260	[24]
$Sr_3Tb(PO_4)_3$	217–220;	251–254	[22]

The VUV excitation spectrum of $La_{0.55}(PO_3)_3$:$Tb_{0.45}^{3+}$ is important. Firstly, the absorption bands of $(PO_3)_3^{3-}$ groups locate at 163 and 174 nm and are consistent with the Xe resonance emission line (147 nm) and the Xe_2 molecular emission band (172 nm), so the absorption efficiency of $La_{0.55}(PO_3)_3$:$Tb_{0.45}^{3+}$ is high under VUV excitation. Secondly, the absorption bands of $(PO_3)_3^{3-}$ groups (174 nm) and La^{3+}–O^{2-} (200 nm) and Tb^{3+} (213 nm) overlap each other, which imply that the energy which is absorbed by the $(PO_3)_3^{3-}$ groups could be efficiently transferred to the 4*f*–5*d* levels of Tb^{3+} and allow the Tb^{3+} to emit green light. Consequently, we could confirm that Tb^{3+}-doped $La(PO_3)_3$ is a potential phosphor under 172 nm excitation.

Fig. 6 shows the emission spectra of $La_{1-x}(PO_3)_3$:Tb_x^{3+} ($0<x\leqslant 0.45$) and $Zn_{1.96}SiO_4$:$0.04Mn^{2+}$ under 172 nm excitation. The strongest emission peak of $La_{1-x}(PO_3)_3$:Tb_x^{3+} ($0<x\leqslant 0.45$) situates at 545 nm and is assigned to the $^5D_4\rightarrow{}^7F_5$ transition of Tb^{3+}. The other peaks at about 487, 583 and 616 nm are associated to the $^5D_4\rightarrow{}^7F_6$, $^5D_4\rightarrow{}^7F_4$ and $^5D_4\rightarrow{}^7F_3$ transitions of Tb^{3+}, respectively. The optimal emission intensity of $La_{1-x}(PO_3)_3$:Tb_x^{3+} is obtained when x reaches 0.45 and is about 71% of commercial phosphor $Zn_{1.96}SiO_4$:$0.04Mn^{2+}$. The chromaticity coordinates of the sample are about (0.343, 0.578), which confirms that $La_{0.55}(PO_3)_3$:$Tb_{0.45}^{3+}$ has the appearance of a pure spectral green. The emission intensity of $La_{1-x}(PO_3)_3$:Tb_x^{3+} ($0<x\leqslant 0.45$) increases with increasing

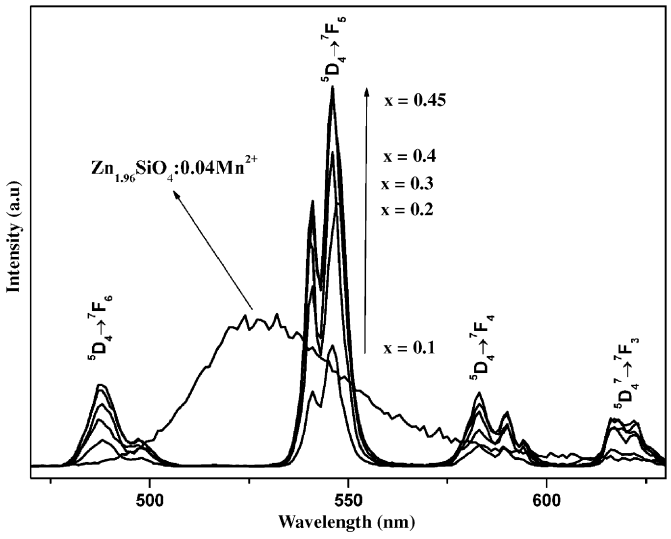

Fig. 6. Emission spectra of $La_{1-x}(PO_3)_3$:Tb_x^{3+} ($0<x\leqslant 0.45$) and $Zn_{1.96}SiO_4$:$0.04Mn^{2+}$ under 172 nm excitation.

the Tb^{3+} concentration. The similar phenomenon has also been observed in the emission spectra of $La_{1-z}P_3O_9:Eu_z^{3+}$ ($0<z\leqslant 1$) [4]. The emission intensity of $La_{1-z}P_3O_9:Eu_z^{3+}$ ($0<z\leqslant 1$) increase linearly and no concentration quenching is observed [4], which indicates that the quenching concentration of rare-earth ions such as Tb^{3+} in $La(PO_3)_3$ would be high. The reason for this phenomenon has not been found, maybe result from the one-dimensional structure of $La(PO_3)_3$ and the big distance between La^{3+} ions. More detailed work is required. However, the emissive intensity of $La_{1-x}(PO_3)_3:Tb_x^{3+}$ is decreased when $x>0.45$. The decreasing intensity could relate to $Tb(PO_3)_3$ because $Tb(PO_3)_3$ appears as the second phase when $x>0.45$ shown in Fig. 2. In order to confirm this conjecture, $Tb(PO_3)_3$ is prepared and its VUV excitation spectrum is measured.

The VUV excitation spectrum of $Tb(PO_3)_3$ (curve *b*) is shown in Fig. 7. The VUV excitation spectrum of $La_{0.55}(PO_3)_3:Tb_{0.45}^{3+}$ (curve *a*) is also plotted for comparison. Four broad bands with the maxima at 158, 171, 210 and 247 nm are observed in the excitation spectrum of $Tb(PO_3)_3$. The bands at 158 and 171 nm could correspond to the absorption of $(PO_3)_3^{3-}$ groups. That is because the anionic group of $Tb(PO_3)_3$ is similar to that of $La(PO_3)_3$ and is composed of three corner-sharing P–O tetrahedra [10,27]. According to Fig. 5, the bands at 210 and 249 nm are assigned to the spin-allowed and spin-forbidden 4*f*–5*d* transition of Tb^{3+}, respectively.

Comparing the excitation spectrum of $La_{0.55}(PO_3)_3:Tb_{0.45}^{3+}$ (curve *a*) with that of $Tb(PO_3)_3$ (curve *b*), we can find that the excitation intensity of $La_{0.55}(PO_3)_3:Tb_{0.45}^{3+}$ is higher in VUV region, which indicates that the absorption efficiency of $La_{0.55}(PO_3)_3:Tb_{0.45}^{3+}$ is superior to that of $Tb(PO_3)_3$ under VUV excitation. Therefore, the emission

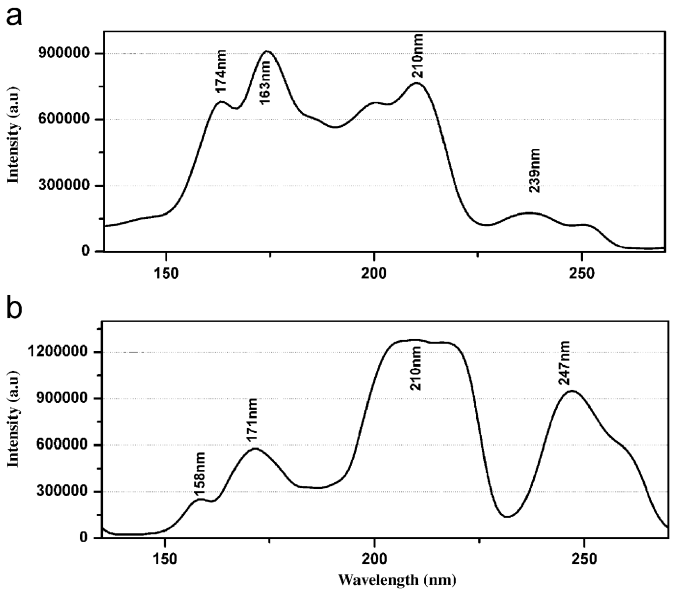

Fig. 7. Excitation spectra of $Tb(PO_3)_3$ (curve *b*, $\lambda_{em}=547$ nm) and $La_{0.55}(PO_3)_3:Tb_{0.45}^{3+}$ (curve *a*, $\lambda_{em}=545$ nm).

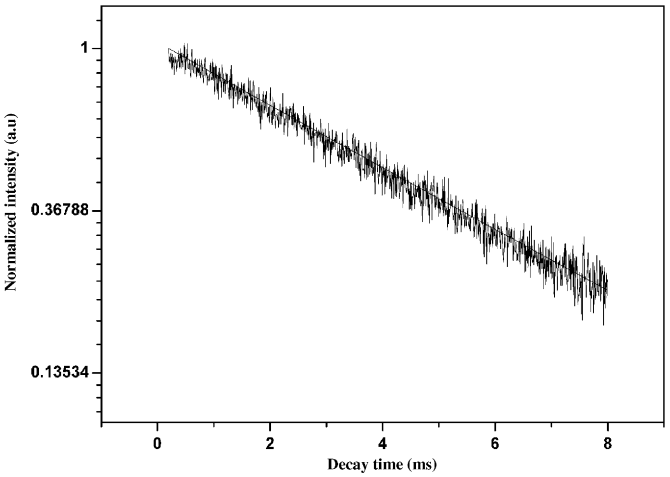

Fig. 8. The decay curve of $^5D_4$–$^7F_5$ transition of Tb^{3+} in $La_{0.55}(PO_3)_3:Tb_{0.45}^{3+}$($\lambda_{ex}=172$ nm).

intensity of $La_{1-x}(PO_3)_3:Tb_x^{3+}$ ($x>0.45$) decreases when the samples become the mixtures of $La(PO_3)_3$ and $Tb(PO_3)_3$.

Fig. 8 shows the decay curve of $^5D_4$–$^7F_5$ transition of Tb^{3+} in $La_{0.55}(PO_3)_3:Tb_{0.45}^{3+}$ under 172 nm excitation. According to the experimental data, the decay curve can be well fitted by single exponential equation. The decay time extracted from the fitted curve is about 4.47 ms (the time to decay $1/e$ of the original intensity).

4. Conclusions

$La_{1-x}(PO_3)_3:Tb_x^{3+}$ ($0<x\leqslant 0.6$) and $Tb(PO_3)_3$ were prepared by solid-state reaction. The VUV excitation spectra of $La_{0.55}(PO_3)_3:Tb_{0.45}^{3+}$ and $Tb(PO_3)_3$ and the emission spectra of $La_{1-x}(PO_3)_3:Tb_x^{3+}$ ($0<x\leqslant 0.45$) were investigated. The excitation spectra indicate that the absorption of $(PO_3)_3^{3-}$ groups in $La_{0.55}(PO_3)_3:Tb_{0.45}^{3+}$ locate at 163 and 174 nm, and the absorption of $(PO_3)_3^{3-}$ groups in $Tb(PO_3)_3$ situate at 158 nm and 171 nm. $La_{0.55}(PO_3)_3:Tb_{0.45}^{3+}$ can efficiently absorb the VUV excited energy and transfer it from the $(PO_3)_3^{3-}$ groups to Tb^{3+} due to the band overlapping of $(PO_3)_3^{3-}$ groups and La^{3+}–O^{2-} and Tb^{3+}.

Under 172 nm excitation, the optimal PL intensity is obtained when x reaches 0.45 and is about 71% of commercial phosphor $Zn_{1.96}SiO_4:0.04Mn^{2+}$ with chromaticity coordinates of (0.343, 0.578) with a decay time of about 4.47 ms.

Acknowledgments

This work was supported by Program for New Century Excellent Talents in University of China (NCET, 04-0978) and Chinese Specialized Research Fund for the Doctoral Program of Higher Education (SRFDP, 20040730019).

References

[1] R.P. Rao, J. Lumin. 113 (2005) 271–278.
[2] E. Nakazawa, F. Shiga, J. Lumin. 15 (1977) 255–259.
[3] H.B. Liang, Y. Tao, Q. Su, S.B. Wang, J. Solid State Chem. 167 (2002) 435–440.
[4] D. Wang, Y.H. Wang, L.L. Wang, J. Electrochem. Soc. 154 (2007) J32–J35.
[5] X. Wu, H. You, et al, Mater. Res. Bull. 37 (2002) 1531–1538.
[6] H.B. Liang, Y. Tao, Q.H. Zeng, H. He, S.B. Wang, X.Y. Hou, W. Wang, Q. Su, Mater. Res. Bull. 38 (2003) 797–805.
[7] D. Wang, Y.H. Wang, Mater. Sci. .Eng. B. 133 (2006) 218–221.
[8] H.Y.P. Hong, Acta Cryst. B 30 (1974) 468–474.
[9] M. Buijs, G. Blasse, J. Lumin. 39 (1988) 323–334.
[10] J. Matuszewski, J. Kropiwnicka, T. Znamierowska, J. Solid State Chem. 75 (1988) 285–290.
[11] H.S. Kiliaan, F.P. Van Herwijhen, G. Blasse, J. Solid State Chem. 74 (1988) 39–46.
[12] A. Jouini, M. Férid, J.C. Gacon, L. Grosvalet, A. Thozet, M. Trabelsi-Ayadi, Mater. Res. Bull. 38 (2003) 1613–1622.
[13] P.P. Melnikov, L.N. Komissarova, T.A. Butuzova, Izv. Akad. Nauk SSSR,, Neorg. Mater. 17 (1981) 2110–2112.
[14] J.M. Sung, S.E. Lin, W.C.J. Wei, J. Eur. Ceram. Soc. 27 (2007) 2605–2611.
[15] H. Yang, C. Li, H. He, G. Zhang, Z. Qi, Q. Su, J. Lumin. 124 (2007) 235–240.
[16] C. Wu, Y.H. Wang, W.J. Liu, J. Solid State Chem. 179 (2006) 4047–4051.
[17] B. Vengala Rao, U. Rambabu, S. Buddhudu, Phys. B. 391 (2007) 339–343.
[18] R.D. Shannon, Acta Crystallogr. A 32 (1976) 751–767.
[19] S. Saito, K. Wada, R. Onaka, J. Phys. Soc. Jpn. 37 (1974) 711–715.
[20] U. Sasum, M. Kloss, A. Rohmann, L. Schwarz, D. Heberland, J. Lumin. 72-74 (1997) 255–256.
[21] H. Liang, Q. Zeng, Y. Tao, S. Wang, Q. Su, Mater. Sci. Eng. B 98 (2003) 213–219.
[22] H. Liang, Y. Tao, J. Xu, H. He, H. Wu, W. Chen, S. Wang, Q. Su, J. Solid State Chem. 177 (2004) 901–908.
[23] W. Di, J. Chen, X. Wang, B. Chen, Chem. Lett. 33 (2004) 1448–1449.
[24] Z.F. Tian, H.B. Liang, H.H. Lin, Q. Su, B. Guo, G.B. Zhang, Y.B. Fub, J. Solid State Chem. 179 (2006) 1356–1362.
[25] C.J. Duan, W.F. Li, X.Y. Wu, H.H. Chen, X.X. Yang, J.T. Zhao, Y.B. Fu, Z.M. Qi, G.B. Zhang, Z.S. Shi, Mater. Sci. Eng. B 121 (2005) 272–277.
[26] R.T. Wegh, H. Donker, A. Meijerijk, Phys. Rev. B 57 (1998) R2025–R2028.
[27] H.Y.P. Hong, Acta Crystallogr. B 30 (1974) 1857–1861.